Building and Environment 124 (2017) 153–170

Contents lists available at ScienceDirect

Building and Environment

journal homepage: www.elsevier.com/locate/buildenv

# Global sensitivity analysis of an urban microclimate system under uncertainty: Design and case study

Jiachen Mao [a, *], Joseph H. Yang [a], Afshin Afshari [b], Leslie K. Norford [a, **]

[a] Massachusetts Institute of Technology, 77 Massachusetts Avenue, Cambridge, MA 02139, USA
[b] Masdar Institute of Science and Technology, PO Box 54224, Abu Dhabi, United Arab Emirates

ARTICLE INFO

*Article history:*
Received 2 June 2017
Received in revised form
12 July 2017
Accepted 4 August 2017
Available online 7 August 2017

*Keywords:*
Urban microclimate
Urban heat island
Sensitivity analysis
Uncertainty analysis
Urban weather generator

ABSTRACT

Over the last decade, significant efforts have been made to develop sophisticated physics-based urban simulators, given the undeniable need for sustainable-city initiatives to consider the potential impacts of climate change and massive urban growth. Nevertheless, even as a growing number of researchers have expanded their scope to the urban realm, there remain many problems resulting from the complexity of the urban microclimate, such as the Urban Heat Island (UHI) effect. This study is initiated with the intention to account for uncertainty in developing more coherent and integrated strategies concerning the energy and environmental issues in an urban system. The analysis builds upon the previously reported and updated Urban Weather Generator (UWG) to present a deep look into an existing urban microclimate system in Abu Dhabi (UAE). The case-specific baseline information is generated for the UWG and a global regression-based sensitivity analysis using the Monte Carlo technique is performed. Based on 30 candidate inputs covering the meteorological factors, urban characteristics, vegetation variables, and building systems, the uncertainty analysis indicates that the UWG is a fairly robust simulator to approximate the urban thermal behavior in downtown Abu Dhabi for different seasons. The identified significant factors will be the subject of future research to gain a higher resolution of critical urban simulation inputs, thereby providing more informed domain knowledge of the underlying mechanisms driving the microclimatic effect on the energy and environmental performances.

Published by Elsevier Ltd.

## 1. Introduction

Global concern about depletion of non-renewable energy sources and anthropogenic climate change has become increasingly prevalent in recent years [1]. Over the next decade, the United Nations predicts that we need to plan and build new homes for billions of city-dwellers worldwide [2]. This unprecedentedly continuous urbanism, if shaped merely by informal or inadequate policy measures, can potentially lead to worrisome consequences for the built environment, the economy at national or international level, and the life quality of billions of people. In response to the urgency of acting to mitigate these challenges, many governmental administrations have prioritized, among other actions, decarbonizing the energy system and reducing GHG emissions at local and global scales in order to achieve a clean-energy economy [3]. While the magnitude of GHG emissions varies among different cities, the building-related emission is always a key contributor [1]. Urban systems need to be better understood to effectively tackle these problems in existing or new neighborhoods, not only which current sectors may cause the environmental issues but also what future changes may best reduce the energy consumption.

As cities develop, the urban area is characterized by an increase in air temperature compared to the surrounding rural area, a phenomenon called the Urban Heat Island (UHI) effect [4]. Regardless of the inherent uncertainties in predicting future climate and weather patterns, the UHI has been measured and documented throughout the world, including in Washington, DC, New York [5], Vancouver, Marseille [6], London [7], Abu Dhabi [8], etc. In particular, Crawley [9] studied the UHI effect on an office building and suggested that the corresponding energy consumption could be modified between 5% (increase in summer) and 10% (decrease in winter). In order to meet the increasing peak demand in summer, more electricity generation by power plants will lead to higher emissions of VOCs, suspended particulates, and $CO_2$, as well as to aggravation of global warming and formation of harmful smog

* Corresponding author.
** Corresponding author.
*E-mail addresses:* maoj@mit.edu (J. Mao), lnorford@mit.edu (L.K. Norford).

http://dx.doi.org/10.1016/j.buildenv.2017.08.011
0360-1323/Published by Elsevier Ltd.

**Nomenclature**

| | |
|---|---|
| $A_f$ | lateral heat exchange area ($m^2$) |
| $c_p$ | specific heat of air at constant pressure (J $kg^{-1}$ $K^{-1}$) |
| $c_v$ | specific heat of air at constant volume (J $kg^{-1}$ $K^{-1}$) |
| $h_{bld}$ | average building height (m) |
| $H_u$ | sensible heat flux at the surface of the control volume (W) |
| $K_{r,dir}/K_{w,dir}$ | fraction of the direct solar radiation received by the road/wall |
| $Q_{LW,down}$ | down-welling infrared radiation specified in the EPW file (W) |
| $Q_{LW,road}/Q_{LW,roof}/Q_{LW,wall}$ | long-wavelength heat exchange between the atmosphere and the road/roof/wall (W) |
| $R^2$ | coefficient of determination |
| $r_{aspect}$ | aspect ratio |
| $r_{shade}$ | fraction of the road shaded by trees |
| $S_{hor,dir}$ | direct solar radiation on a horizontal surface (W $m^{-2}$) |
| $S_{norm,dir}$ | direct normal solar radiation (W $m^{-2}$) |
| $T_{road}/T_{roof}/T_{wall}$ | surface temperature of the road/roof/wall (K) |
| $u_{ref}$ | reference air velocity (m $s^{-1}$) |
| $V_{CV}$ | control volume ($m^3$) |
| $VF_{i-j}$ | view factor from *i* to *j* |
| $w_r$ | average road width (m) |

*Greek symbol*

| | |
|---|---|
| $\varepsilon_{road}/\varepsilon_{roof}/\varepsilon_{wall}$ | emissivity of the road/roof/wall |
| $\theta_o$ | critical canyon orientation |
| $\theta_{ref}$ | reference potential temperature outside the control volume (K) |
| $\theta_u$ | average potential temperature of the control volume (K) |
| $\lambda$ | solar zenith angle |
| $\rho$ | air density (kg $m^{-3}$) |
| $\sigma$ | Stefan-Boltzmann constant (W $m^{-2}$ $K^{-4}$) |

*Abbreviation*

| | |
|---|---|
| AM | averaged model |
| BTEX | Benzene, Toluene, Ethylbenzene, and m-, p-, o-Xylenes |
| CFD | computational fluid dynamics |
| $CO_2$ | carbon dioxide |
| COP | coefficient of performance |
| DM | detailed model |
| DOE | Department of Energy |
| EPW | EnergyPlus Weather |
| GHG | greenhouse gas |
| HVAC | heating, ventilation, and air conditioning |
| IR | infrared radiation |
| LW | long-wavelength |
| RMSE | root-mean-square error |
| RSM | rural station model |
| SA | sensitivity analysis |
| SHGC | solar heat gain coefficient |
| SRC | standardized regression coefficient |
| SRRC | standardized rank regression coefficient |
| TEB | Town Energy Balance |
| UBL | urban boundary layer |
| UCL | urban canopy layer |
| UCM | urban canopy model |
| UHI | Urban Heat Island |
| UWG | Urban Weather Generator |
| VDM | vertical diffusion model |
| VOC | volatile organic compound |

[10]. There is thus a pressing need for simulation tools to quantify the actual risks caused by the interactions between building thermal behaviors and urban climate changes, as well as to help building designers, facility managers, and policy makers produce informed decisions for the future.

Currently, there have been great efforts to incorporate the UHI effect into energy and environmental simulations, including mesoscale computational fluid dynamics (CFD) models [11,12], analytical and empirical algorithms [9], and physics-based urban canopy models [13–15]. As different models are developed for different uses, different spatial scales need to be clearly defined and different urban models need to be elaborated in terms of their capabilities to predict corresponding energy and environmental conditions. Although the mesoscale models are regarded as state-of-the-art in atmospheric weather predictions [16], their applications still remain limited due to high computational cost and lack of boundary condition data.

As an alternative, Bueno et al. [17] developed the Urban Weather Generator (UWG) to quickly estimate the UHI effect in the urban canopy layer and produce neighborhood-specific weather files, using the meteorological data measured at weather stations located in an open area outside the city. The UWG can also be considered as an off-line bottom-up model to evaluate the building energy consumption at the neighborhood-to-city scale. It has been validated in Toulouse (France), Basel (Switzerland) [17], Singapore [18], and Boston (USA) [19]. With continuous improvements and updates [20], the UWG has the potential to be a promising urban microclimate simulation engine that shows satisfactory performance with acceptable computational cost.

However, despite these positive developments, urban simulation practice has been applied only to a fraction of new construction and urban morphologies. One recognized obstacle is the discrepancies, sometimes significant, between simulation-predicted and actual measured values [21]. The reason may lie in the fact that a single simulation only evaluates a single point in the parameter space without taking uncertainties into account. Consequently, building designers or city planners often perform manual parametric simulations varying one factor at a time, which is referred to as the local analysis. This is why some cynics would say that "models can be made to conclude anything provided that suitable assumptions are fed into them" [22]. As many inputs in the model are associated with some degree of uncertainty, due to changeable conditions or lack of knowledge about the exact value, sensitivity analysis of model parameters plays an important role in the simulation process in order to achieve valuable information and increase model confidence.

Sensitivity analysis (SA), presented by Saltelli et al. [23], is a measure of the effect of an input on the output. In general, given the input uncertainties, one is able to assess the uncertainty in the model response (uncertainty analysis), and eventually to identify the inputs that contribute most to that uncertainty (sensitivity analysis). Thus, SA can be of tremendous help in subsequent model analysis, including simulation-based optimization [24], meta-model analysis [25], automatic model calibration [26], etc. The SA

methods can generally be divided into local and global approaches [23]. The local methods require fewer computations but are ill-suited for complex systems. The global methods are regarded as more versatile to handle non-linear, non-additive, and non-monotonic systems [27,28]. A brief literature review suggests that the global SA has been widely applied in building thermal simulations [29–34]. In addition, some researchers have started to look at the causal factors of urban climate change and heat island effect via parametric studies [6,8,14,15,17,19]. However, to the authors' best knowledge, there is nearly no related work on performing the global SA in urban microclimate models with respect to a large multiplicity of factors. This is because the global SA approaches are so computationally expensive that most urban-scale simulations cannot afford them. Fortunately, with acceptable performances and unprecedentedly low computational requirements, the UWG enables a first step toward the exploration of the global design space with various input parameters in urban simulations.

This paper presents the application of a global SA method to the UWG model of an existing urban area located in Abu Dhabi (UAE). The aim of the present study is to determine the relative impacts of input parameters on estimates of the urban air temperature and urban energy consumption. Section 2 introduces the mechanism and updated features of the UWG for urban microclimate simulations. Section 3 illustrates the establishment of a baseline model for the subsequent Monte Carlo uncertainty/sensitivity analysis detailed in Section 4. Finally, results and discussions of the current analysis are provided in Section 5, and the corresponding conclusions are given in Section 6. This study is expected to be useful in understanding the microclimate in and around urban areas. The proposed approach has the potential to improve the way cities are designed and operated in the near future.

## 2. Urban weather generator: introduction and update

The urban microclimate strongly depends on the urban surface layer. The latter is determined by the energy balance [35,36] between the received net radiation (both short-wave and long-wave), the sensible and latent heat fluxes transferred to the air, the heat storage in urban structures and the ground, and the anthropogenic heat sources, as shown in Fig. 1(a). The energy-balance characteristics may vary with the city location, built form, urban geometry, surface materials [15,37], etc. Therefore, the UHI effect tends to vary significantly from one location to another, and should be considered as site-specific.

In order to capture the UHI effect and simulate the microclimate condition, the Urban Weather Generator (UWG) was developed by Bueno et al. [17] as a stand-alone program to map a reference weather file to the estimated conditions at a neighborhood scale based on the specific urban area characteristics. The wisdom of the UWG comes from the fact that many communities do not have access to the microclimate information from local experimental measurements and mesoscale simulation results, while the rural meteorological information can be easily found in currently available weather files. Starting with the rural weather data provided in the EPW format and the urban characteristics, the UWG outputs the simulated urban weather data (during either an entire calendar year or just a subset thereof) that can be readily used in the EPW format.

As shown in Fig. 1(b), the UWG consists of four coupled models: the rural station model, the vertical diffusion model, the urban boundary layer model, and the urban canopy-building energy model. Detailed physical mechanisms of these models can be found in Refs. [17,39]. Originally written in MATLAB, the latest update of the UWG program further includes XML [19] and Excel [20] interfaces to allow flexibility in input formats of the urban characteristics. Since the previous version in 2014 [18], the UWG has been updated, especially for the urban boundary layer model and the urban canopy-building energy model, with the purpose of making it more physically sound and more capable to handle increasingly detailed building definition. Major updated features of the current UWG are described below.

### 2.1. Urban canopy model

Based on the Town Energy Balance (TEB) scheme proposed by Masson [13], the UWG maps the 3D urban geometry to a 2D canyon model consisting of a wall, roof, and road, representative of the average urban characteristics. While the previous version bounded the canyon volume by twice the building height, the urban boundary layer (UBL) in the new version extends down to the top of the building. All heat released from the roof is assumed to directly enter the UBL. This makes the formulation more consistent with the original TEB scheme.

The solar radiation in the new version is also updated for numerical stability. According to Masson [13], their fractions are given by:

$$K_{w,dir} = \min\left(\frac{w_r}{h_{bld}}\left(\frac{1}{2} - \frac{\theta_0}{\pi}\right) + \frac{1}{\pi}\tan(\lambda)(1 - \cos(\theta_0)),\ 1\right) \tag{1}$$

$$K_{r,dir} = \min\left(\frac{2\theta_0}{\pi} - \frac{2}{\pi}\frac{h_{bld}}{w_r}\tan(\lambda)(1 - \cos(\theta_0)),\ 1 - 2r_{aspect}K_{w,dir}\right) \tag{2}$$

where $K_{w,dir}$ is capped to 1 as the sun approaches the horizon.

While Masson defined these terms to scale the direct solar radiation received by a horizontal surface, the value specified in a standard EPW file is the direct normal radiation, namely the solar radiation received by a surface perpendicular to the sunlight direction. This indicates that the previous model had a slightly excessive solar gain. Thus, the direct solar radiation in the new version of UWG is modified as:

$$S_{hor,dir} = S_{norm,dir}\cos(\lambda) \tag{3}$$

In terms of the infrared radiation (IR) exchange, the previous version seemed to over-estimate the IR absorption by bodies of air [38]. To correct this over-estimation, the air is assumed to be essentially transparent to the long-wavelength (LW) radiation emitted from its boundary surfaces. This assumption has been validated with MODTRAN simulations [20], showing that the IR absorption of the air is almost negligible for the thick air bodies (around 1 km) considered in UWG. Thus, the net LW heat exchanges with the atmosphere for the roof, wall, and road are given as:

$$Q_{LW,roof} = \varepsilon_{roof}\left(Q_{LW,down} - \sigma T_{roof}^4\right) \tag{4}$$

$$Q_{LW,wall} = \varepsilon_{wall}VF_{wall-sky}\left(Q_{LW,down} - \sigma T_{wall}^4\right) + \sigma\varepsilon_{road}\varepsilon_{wall}VF_{wall-road}(1 - r_{shade})\left(T_{road}^4 - T_{wall}^4\right) \tag{5}$$

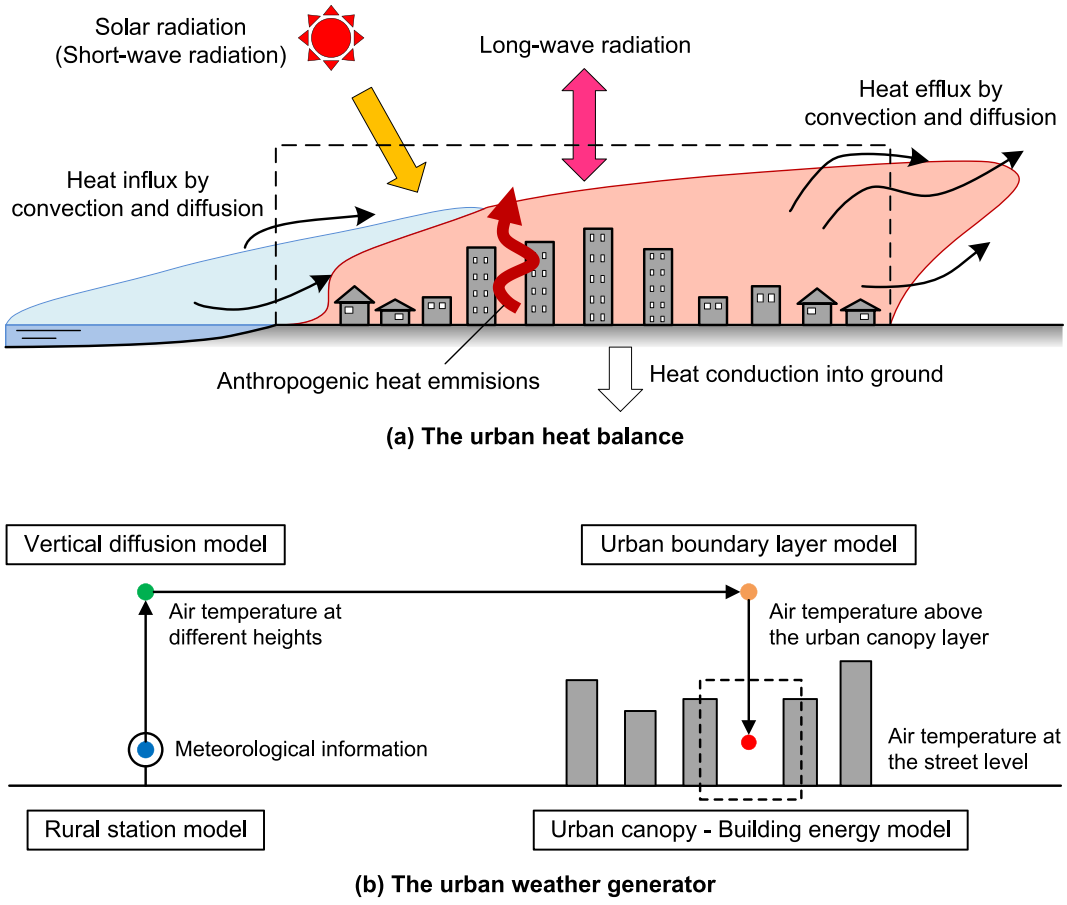


**Fig. 1.** Concept of the urban microclimate environment: (a) Heat balance of urban surface layer (mainly from Ooka et al. [36]); (b) The urban weather generator (mainly from Bueno [17]).

$$Q_{LW,road} = \varepsilon_{road} VF_{road-sky}(1 - r_{shade})\left(Q_{LW,down} - \sigma T_{road}^4\right) + \sigma\varepsilon_{road}\varepsilon_{wall} VF_{road-wall}(1 - r_{shade})\left(T_{wall}^4 - T_{road}^4\right) \quad (6)$$

where $Q_{LW,down}$ has accounted for the radiative effect due to the water vapor and carbon dioxide contained in the UBL.

Since the latent heat exchange between the four coupled models was not fully considered, we decide to remove the humidity calculation for canyon in the new version of UWG. This calculation requires consideration of the moisture from vegetation, soil, combustion, nearby bodies of water, etc., and these components have not been precisely modeled in the current UWG. It is also worth noting that the latent heat balance in the urban canyon has not been formally validated [17,18]. Thus, the absolute humidity in the rural area is assumed the same as that in the urban area, and is then used to calculate the relative humidity for the generated EPW file. When accounting for the solar radiation received by the vegetation, we only consider its sensible portion in the energy balance, subtracting a prescribed latent-energy fraction.

When the urban weather file is generated, the calculated canyon wind speed is included, instead of the rural wind speed used by previous versions. The calculation is detailed in the appendixes of Refs. [17,18]. In addition, the updated UWG incorporates a user-specified hourly schedule for the traffic-generated heat flux, as a counterpart to the schedules defined in the building energy model, to make the simulated diurnal microclimate profile more accurate. Finally, the new version of UWG reads the soil temperatures from the EPW file, and uses these values as the boundary condition to obtain the road layer temperature profile. It is also worth noting that the road elements in the new version are divided into thinner layers (with maximum of 5 cm) so that the surface temperature fluctuation can be captured more precisely.

### 2.2. Urban boundary layer model

The urban boundary layer (UBL) model solves an energy balance for a control volume above the urban canopy layer (UCL) where the boundary conditions can be imposed [39]. The UBL is considered as a region of well-mixed and isothermal air below a capping inversion.

As explained in Subsection 2.1, the IR portion of the energy exchange added in 2014 [18] is now removed. Thus, the energy balance of the current UBL model remains the same as the original version in 2012 [39], defined as:

$$V_{CV}\rho c_v \frac{d\theta_u}{dt} = H_u + \int u_{ref}\rho c_p\left(\theta_{ref} - \theta_u\right)dA_f \quad (7)$$

where the term on the LHS stands for the thermal inertia of the control volume, and the second term on the RHS stands for the advection effect.

The heat exchange at top of the control volume is assumed negligible when the vertical profile of the potential temperature provided by the vertical diffusion model is constant. So, the energy

balance of the UBL model is driven only by the heat flux from the bottom or the lateral sides of the volume surface.

The advection effect is driven by either the horizontal flow or the radial urban-breeze circulation where the wind direction is not taken into account. Therefore, the rural weather data seems applicable to large concentric regions surrounding the urban area [40].

### 2.3. Building energy model

The building energy model approximates the heat balance of the indoor air temperature for each building. For simplicity, the air temperature is assumed uniform within the entire building envelope. As a result, the UWG can capture the building energy operations and calculate the waste heat emissions from HVAC systems, which are the potentially significant sources of heat in the energy balance of an urban canyon.

Whereas the old version only specified the total internal heat load in buildings, the new UWG takes into account the variation in the types of heat loads. As shown in Table 1, the updated UWG treats the convective, latent, and radiant heat loads separately. The convective and latent heat exchange is added directly into the indoor air heat balance, while the radiant heat flux is received by the ceiling and floor. The view factors from lights and occupants to the ceiling and floor are assumed close to unity.

To simplify the estimation of various building types at a neighborhood scale, commercial building reference data is imported from the US DOE online database [42] into a spreadsheet associated with UWG. This allows the users to specify the building types that make up the urban area, instead of modeling all the buildings individually. Accordingly, the updated UWG simulates the hourly schedules of occupancy, lighting, and equipment loads for each building type using the default values provided in the DOE reference building database, with flexible options for user customization. The goal is a better estimation of the building energy use pattern at the urban scale and the temporal sensible heat fluxes released into the surrounding environment. In addition, we consider a single building zone with a generic thermal mass and use the multi-zone-weighted average to calculate the internal heat gain. The simplified building models have been validated against the original models in Ref. [20].

For the heating mechanism in the updated version, the internal heat gain is added into the building control volume based on the heating requirement, instead of based on the supply air temperature and mass flow rate. On the other hand, the cooling demand is determined by a psychrometric model based on the apparatus dew point. If the energy demand is greater than the system capacity, the system capacity is then used to calculate the supply air temperature.

In order to properly size the building elements, detailed information for the case study is determined according to local summaries and then is substituted into the DOE reference building database. As for the thermal properties of the building envelope, if the insulation layer is too thin (less than 1 cm), it will not be modeled in the structural element to avoid solver instability. Such omission will not significantly affect the thermal characteristics of the structure. However, the surface optical properties, such as the albedo and emissivity, are still taken into account.

Finally, while the previous version calculated the waste heat based on the total building energy consumption, the updated version treats the waste heat in more detail. The energy consumed by lights and equipment is considered as the heat flux received by either indoor air or internal surfaces, eventually merging with the canyon air through windows and walls. The waste heat added directly into the canyon is calculated based on the HVAC-related waste heat (with a predetermined fraction), as well as the waste heat from hot water usage and gas consumption.

## 3. Baseline urban design

### 3.1. Case study in Abu Dhabi

In this section, a baseline model is established using the new version of UWG for a typical district in downtown Abu Dhabi (UAE). Abu Dhabi has been developed rapidly over the past 60 years. Its climate is characterized by a very hot summer from July to September and a mild winter from December to February. The city experiences an environment with generally high temperatures and insufficient rainfall throughout the year. The Köppen climate classification subtype for Abu Dhabi is BWh (tropical and subtropical desert climate).

This case study was conducted in District E3, which is representative of many other downtown districts in Abu Dhabi. The total area of District E3 is about 193,351 $m^2$. As shown in Fig. 2, there is a row of high-rise residential, office, and hotel buildings on the outer borders surrounding a number of medium- and low-rise buildings in the inner part. In total, 70 buildings are considered in the baseline model, including 59 residential buildings, five office buildings, three hotels, one mosque, one school, and one hospital. In general, the buildings built in the 1990s have smaller window-to-wall ratios, while the buildings built after 2000 are mostly glazed over the façade. This makes Abu Dhabi an interesting case with heterogeneous building forms located in a tropical or subtropical climate zone.

The parameters used for establishing the baseline model can be categorized into four groups: meteorological factors, urban characteristics, vegetation variables, and building systems. Since the detailed data collection efforts on building properties would become impractical at the urban scale, it is necessary to abstract a building stock into “building archetypes.” While such division is of tremendous importance for modeling reliability, the process usually remains *ad hoc* based on generic assumptions. In our case study, the descriptions of the baseline model are based on careful selections of typical design and construction with corresponding data taken from the Abu Dhabi Municipality (via personal contact) and prevailing engineering practices [8,17,18,39,42–44]. A summary of the key input parameters is shown in Tables 2 and 3. The structural elements of the DOE reference buildings based on the Miami climate are modified according to the current building descriptions, since the climate in Miami is quite similar to that in Abu Dhabi.

**Table 1**
Fractions of the internal heat loads.

| | Occupancy load | Equipment load | Lighting load | Added to |
|---|---|---|---|---|
| Convective fraction | 0.5 | 0.5 | 0.3 | Air |
| Latent fraction | 0.3 | 0 | 0 | Air |
| Radiant fraction | 0.2 | 0.5 | 0.7 | Mass |

Note: The fraction values are selected based on ASHRAE Handbook – Fundamentals [41].

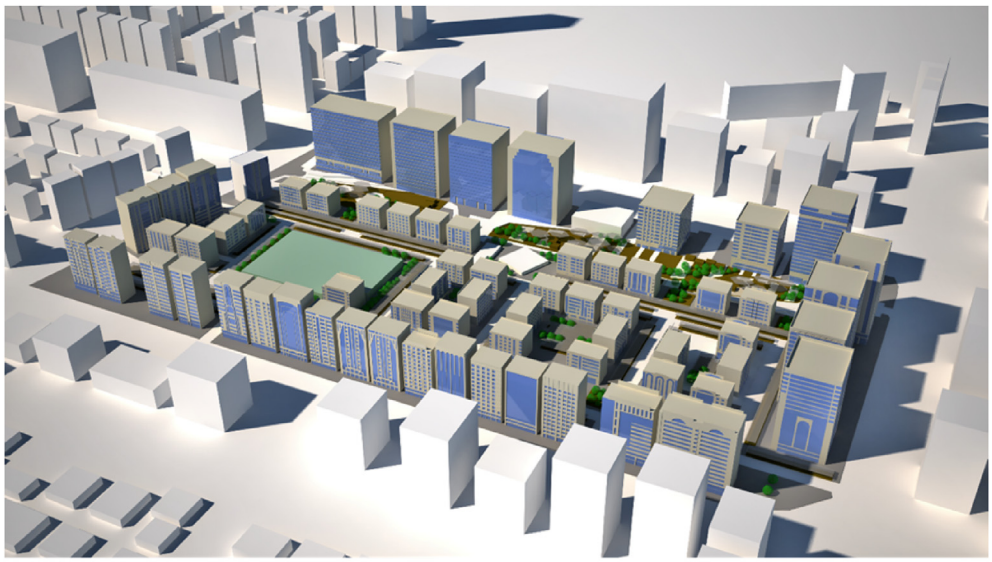

(a) District E3 in downtown Abu Dhabi (3D model)

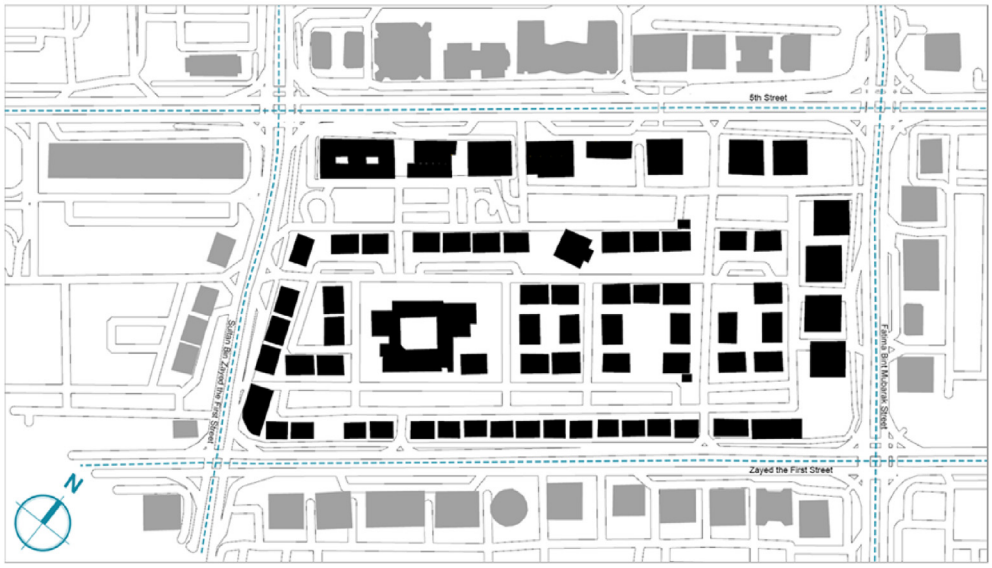


(b) District E3 in downtown Abu Dhabi (site view)

**Fig. 2.** District E3 in downtown Abu Dhabi: (a) 3D model created from Rhinoceros; (b) Site view created from Google Maps.

### 3.2. Model of anthropogenic heat flux

In urban studies, anthropogenic heat flux is defined as the heat released due to human activities [4]. According to Sailor [45], it generally includes the heat from building operation, traffic vehicles, and human metabolism.

A methodology is proposed to evaluate the aggregated effect of building energy models on the outdoor microclimate conditions in the subsequent uncertainty/sensitivity analysis. The underlying expectation is that the average building in a specific urban area is more thermally homogeneous and generic than each particular building. Two models of District E3 with different levels of detail are compared via UWG. The first model, referred to as the detailed model (DM), includes the exact information for the six building archetypes extracted from available resources. The second model, referred to as the averaged model (AM), maintains the assumptions of the building energy model but considers only one building archetype using weighted average values. The key parameters of building geometry, energy load, and HVAC system are all set as weighted averages based on corresponding area or volume. We assume that the schedules for each building prototype cannot be averaged and thus remain unchanged. This method is adopted only if the objective is to evaluate the overall energy consumption of a neighborhood area, rather than the energy performance of a specific building. Tables 3 and 4 summarize the parameters in DM and AM, respectively.

In the meantime, there is an ongoing research project working exclusively on quantifying the traffic-related anthropogenic heat in District E3 [46], since the outdoor metabolic heat is negligible and the building-related waste heat can be calculated by the UWG. The novelty of the method lies in the assumption that the air quality measurements can be a proxy for traffic intensity. In particular, the BTEX (Benzene, Toluene, Ethylbenzene, and m-, p-, o-Xylenes) concentration levels appear strongly correlated with the traffic intensity [46].

The normalized diurnal profiles of the traffic intensity were

**Table 2**
Inputs of the UWG used in the baseline model with field data from District E3 in Abu Dhabi.

| Parameter | Setting |
|---|---|
| *General information* | |
| Location | Abu Dhabi |
| Latitude | 24.490° |
| Longitude | 54.366° |
| Simulation time-step | 300 s |
| Weather data time-step | 3600 s |
| Simulation period | 10/01/2016–10/07/2016 |
| | 11/01/2016–11/07/2016 |
| | 12/01/2016–12/07/2016 |
| *Meteorological factors* | |
| Daytime urban boundary layer height | 700 m |
| Nighttime urban boundary layer height | 80 m |
| Reference height of the VDM | 150 m |
| RSM temperature reference height | 10 m |
| RSM wind reference height | 10 m |
| Circulation coefficient | 1.2 |
| UCM-UBL exchange coefficient | 0.3 |
| Heat flux threshold for daytime conditions | 200 W $m^{-2}$ |
| Heat flux threshold for nighttime conditions | 50 W $m^{-2}$ |
| Minimum wind velocity | 0.1 m $s^{-1}$ |
| Rural average obstacle height | 0.1 m |
| *Urban characteristics* | |
| Average building height | 35 m |
| Fraction of waste heat into canyon | 0.3 |
| Building density | 0.24 |
| Vertical-to-horizontal ratio | 2.2 |
| Urban area characteristic length | 1000 m |
| Road albedo | 0.165 |
| Pavement thickness | 1.25 m |
| Traffic sensible anthropogenic heat (peak) | 19.6 W $m^{-2}$ |
| Traffic latent anthropogenic heat (peak) | 2.0 W $m^{-2}$ |
| *Vegetation variables* | |
| Urban vegetation coverage | 0.01 |
| Urban tree coverage | 0.01 |
| Start month of vegetation participation | January |
| End month of vegetation participation | December |
| Vegetation albedo | 0.25 |
| Latent fraction of grass | 0.6 |
| Latent fraction of tree | 0.7 |
| Rural vegetation coverage | 0.01 |

Note: Detailed physical definition of the parameters can be found in Refs. [17,39]. In particular, Ref. [17] illustrates the parameters in the rural station model and the urban canopy-building energy model, while Ref. [39] illustrates the parameters in the vertical diffusion model and the urban boundary layer model.

derived using the BTEX concentrations measured in a downtown air quality monitoring station near District E3 during calendar year 2012. We neglect the seasonal dependence and focus on the variance on a daily basis, since the diurnal average BTEX profile is not sensitive to seasons. As shown in Fig. 3, the Friday profile is quite different from the workday profile, whereas Saturdays present wide similarities with workdays. There are two peaks at 9 a.m. and 10 p.m. and one minimum at 5 a.m. in the workday diurnal profile. The Friday profile also peaks at 10 p.m., while the high values persist during the nighttime. Such differences can be explained by cultural and climatic reasons. In Abu Dhabi, it is worth noting that the weekend is Friday and Saturday; Friday is the weekly Muslim holy day, a day of public worship.

The normalized profile has been calibrated using either a bottom-up method based on high-resolution satellite images of the traffic intensity, or a top-down method based on average macro-economic and demographic variables. Both methods have been applied and the results are quite similar. The peak traffic sensible anthropogenic heat load for the diurnal profile is 19.6 W/$m^2$, based on the full site. This is quite consistent with the result produced by Quah and Roth [47] in Singapore. The peak latent heat load due to motorized traffic is estimated to be 2.0 W/$m^2$.

**Table 4**
Building parameters for the averaged model (AM) in the UWG.

| Building parameter | Weighted average |
|---|---|
| Glazing ratio | 0.48 |
| Wall U-value (W $m^{-2}$ $K^{-1}$) | 2.50 |
| Roof U-value (W $m^{-2}$ $K^{-1}$) | 0.70 |
| Window U-value (W $m^{-2}$ $K^{-1}$) | 3.25 |
| Window SHGC | 0.58 |
| Infiltration rate (ACH) | 0.60 |
| Lighting load density (W $m^{-2}$) | 10 |
| Equipment load density (W $m^{-2}$) | 13 |
| Occupancy density ($m^2$ $person^{-1}$) | 19 |
| Indoor air set point (°C) | 22 |
| Chiller COP | 2.5 |

Note: The wall-, window-, and roof-related parameters are averaged based on the wall, window, and roof area, respectively. The internal heat gains are averaged based on the floor area. The infiltration level is averaged based on the building volume.

### 3.3. Reference and sensor data

The rural reference weather data used for the baseline model is taken from the Masdar Institute Field Station, an isolated laboratory building in Masdar City. The station is located near the Abu Dhabi airport, 28 km from the downtown area. The rural station is basically surrounded by deserts connecting Abu Dhabi, Dubai, and Al Ain. Due to regular maintenance to ensure data quality, the measured data during calendar year 2016 is used for running the UWG. As shown in Fig. 4, Abu Dhabi has a maximum temperature in August 2016 (about 47.3 °C) and a minimum temperature in

**Table 3**
Building parameters for the detailed model (DM) in the UWG.

| Building parameter | Residential | Hotel | Office | Mosque | School | Hospital |
|---|---|---|---|---|---|---|
| Total floor area ($m^2$) | 382,086 | 99,666 | 140,886 | 2070 | 15,159 | 10,589 |
| Glazing ratio | 0.39 | 0.75 | 0.72 | 0.11 | 0.34 | 0.90 |
| Wall U-value (W $m^{-2}$ $K^{-1}$) | 2.70 | 2.27 | 1.71 | 2.70 | 2.70 | 1.71 |
| Roof U-value (W $m^{-2}$ $K^{-1}$) | 0.74 | 0.74 | 0.53 | 0.74 | 0.74 | 0.53 |
| Window U-value (W $m^{-2}$ $K^{-1}$) | 3.88 | 2.40 | 2.40 | 3.88 | 3.88 | 2.40 |
| Window SHGC | 0.75 | 0.36 | 0.36 | 0.75 | 0.75 | 0.36 |
| Infiltration rate (ACH) | 0.75 | 0.50 | 0.30 | 0.75 | 0.75 | 0.20 |
| Lighting load density (W $m^{-2}$) | 8 | 10 | 12 | 8 | 15 | 15 |
| Equipment load density (W $m^{-2}$) | 12 | 13 | 15 | 5 | 10 | 15 |
| Occupancy density ($m^2$ $person^{-1}$) | 25 | 10 | 10 | 10 | 8 | 15 |
| Indoor air set point (°C) | 22 | 22 | 22 | 22 | 22 | 22 |
| Chiller COP | 2.5 | 2.5 | 2.5 | 2.5 | 2.5 | 2.5 |

Note: The values are determined based on the corresponding data taken from local building design/energy codes provided by the Abu Dhabi Municipality (via personal contact), the on-site survey, and the prevailing engineering practices [8,42–44].

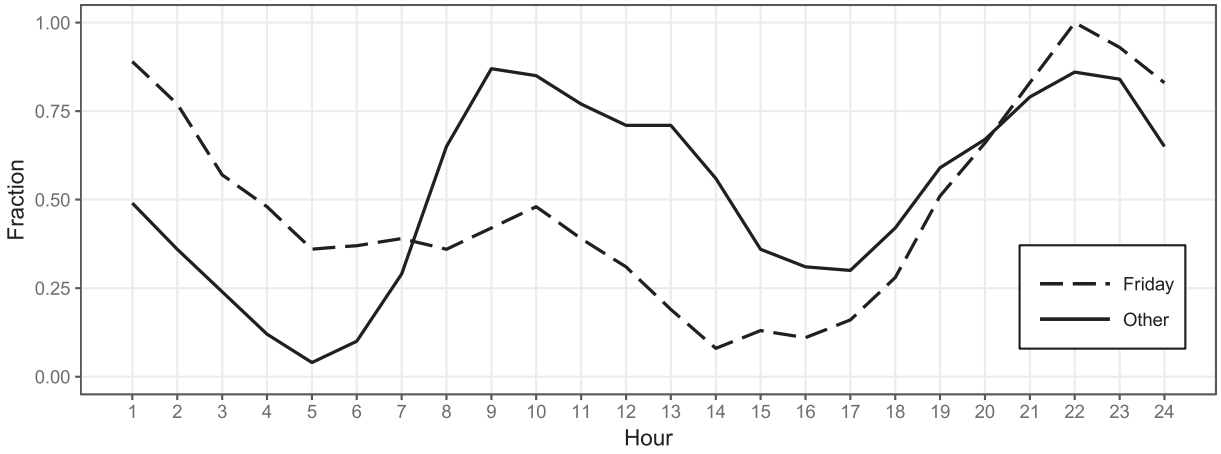


**Fig. 3.** Normalized diurnal profile of the average traffic intensity in Abu Dhabi based on the BTEX concentration (mainly from Afshari et al. [46]).

February 2016 (about 8.7 °C).

Temperature observations from installed urban sensors are compared with the predicted values by the UWG baseline model. In fall 2016, several arrays of sensors were attached to six lamp poles in District E3 at different sites, representing a range of land usages, morphological parameters, building operations, etc. Each sensor array consists of temperature measurements (at 3, 4, 5.5, 7, and 8.5 m), relative humidity measurements (at 3 m), and wind measurements (at 6 m, only available in four of the six stations). The sensors were inspected against each other before deployment to ensure relative accuracy of readings. This study uses the data from three of the calibrated sensors that present consistent performances. The corresponding locations in (latitude, longitude) of the three sensors are (24.4902°, 54.3654°), (24.4894°, 54.3663°), and (24.4907°, 54.3660°). In particular, the temperature observations at 8.5 m are selected for the subsequent comparison.

### 3.4. Prediction of urban air temperature

Fig. 5 compares the weekly-average profiles of rural and urban air temperature calculated by the model from October to December 2016. The diurnal pattern of UHI is characterized by a slightly cooler temperature in the urban area than in the rural area during the late morning, and a relatively warmer temperature from the afternoon to the early morning the next day. The urban-rural temperature difference is more intense in the early morning. This is quite consistent with the results from previous studies [4,17,18]. Generally speaking, due to the aggregate effect of the whole city, the UHI cannot be neglected in Abu Dhabi for the assessment of either thermal comfort or energy consumption.

We can also see that the DM and AM present almost the same profile of the urban air temperature. The differences in the diurnal pattern, computed as the root-mean-square error (RMSE) between the DM and AM, are all about 0.03 °C from October to December. On the other hand, the difference in urban electricity use between the DM and AM can be observed to some extent in Fig. 6, especially during the daytime. The corresponding diurnal differences, computed as the RMSE between the DM and AM, are respectively about 0.52, 0.59, and 0.64 MWh in October, November, and December. Usually there are more cooling demands during the

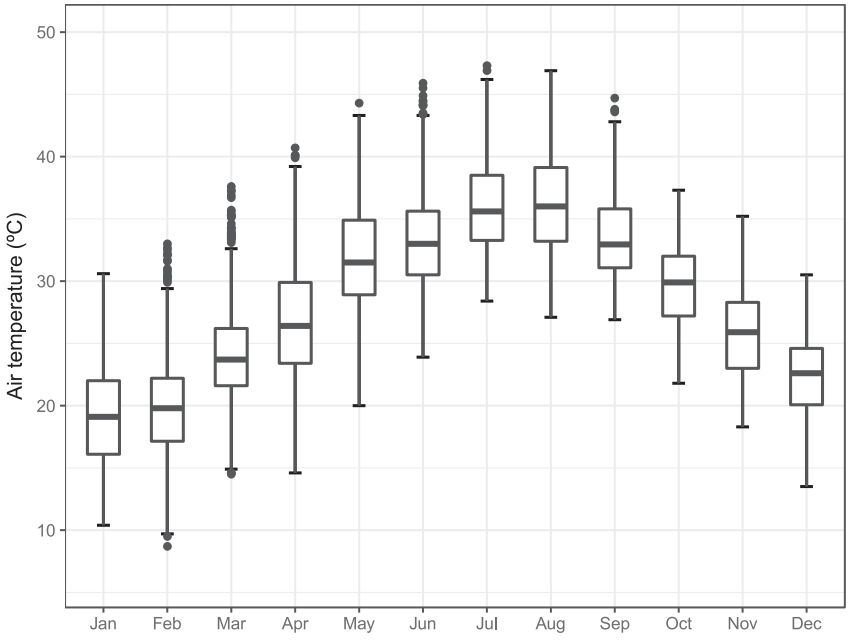


**Fig. 4.** Monthly air temperature measured at the rural station in Abu Dhabi during 2016.

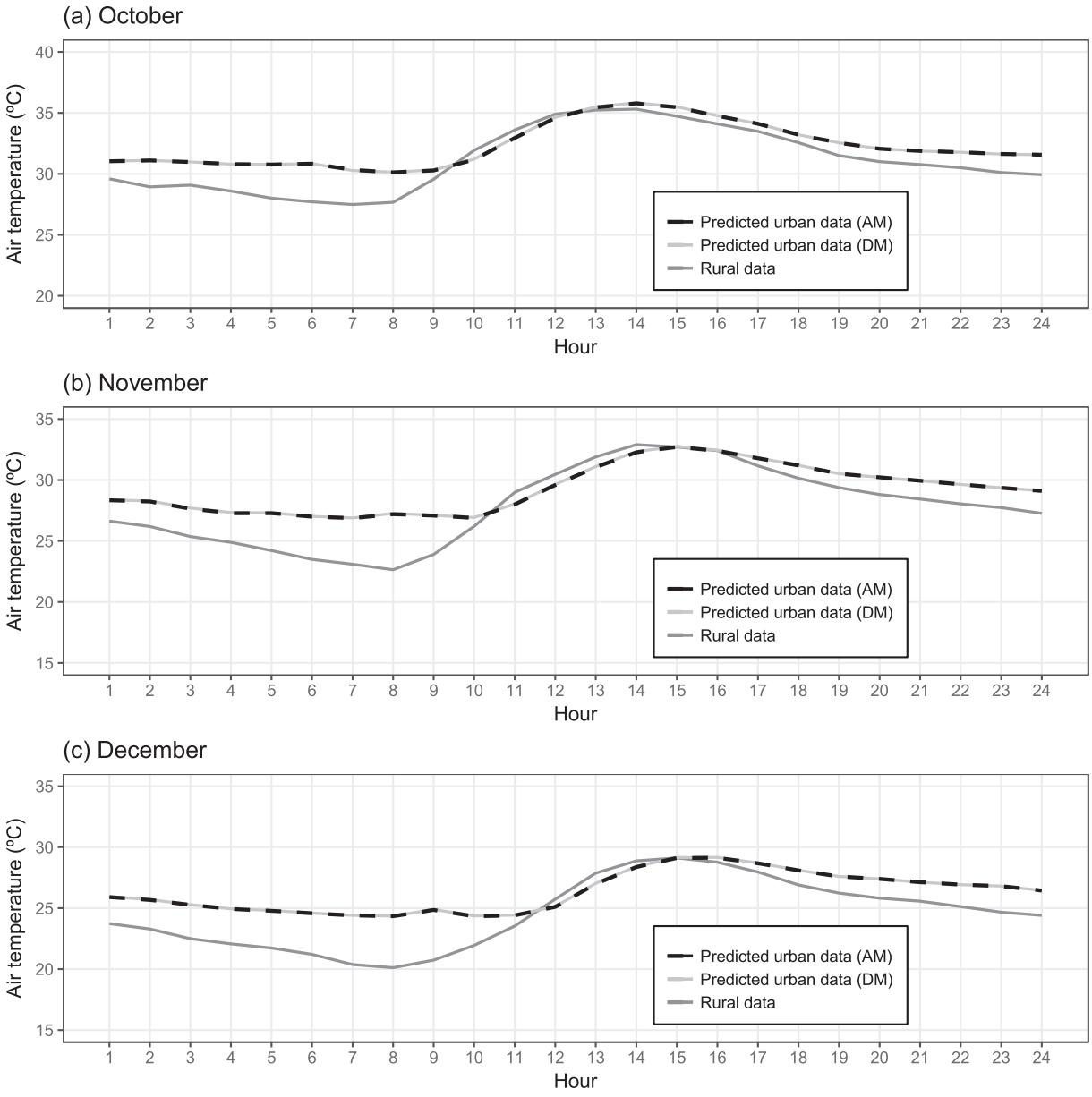


**Fig. 5.** Weekly-average diurnal profiles of the rural and urban outdoor air temperature: (a) Data between October 1 and 7, 2016; (b) Data between November 1 and 7, 2016; (c) Data between December 1 and 7, 2016.

daytime than during the nighttime for Abu Dhabi, resulting in more significant impacts of building-related parameters on the urban energy consumption. Nevertheless, the differences are not very high given the state-of-the-art of urban energy modeling. This justifies the application of the AM in the UWG to assess the aggregated effect of building energy models on the outdoor microclimate conditions in the subsequent analysis.

The capacity of the UWG baseline model with the averaged building energy models to predict the urban outdoor air temperature is evaluated against the observations from October to December 2016, as shown in Fig. 7. To properly describe the air temperature in the whole area of District E3 and to account for the sensor measurement uncertainty, we considered the average and standard deviation of the three sensors. Fig. 7 illustrates that the UWG tends to either over-predict or under-estimate the urban air temperature to some extent in the daytime. In general, the prediction performance is relatively better during the nighttime than during the daytime. Although validation of the electricity use prediction has not been performed—due to our current inability to access such data—we expect to obtain the corresponding meter data and will include such validation in the future. Still, considering the complexity of urban systems, the UWG can roughly capture the UHI pattern and produce some plausible values regarding the urban microclimate condition.

## 4. Parametric simulation and sensitivity analysis

The measurement uncertainty has been taken into account, but not the simulation uncertainty. The next step of the analysis is to find the most influential parameters and to evaluate the effects of their uncertainties on the predicted urban microclimatic performance for different seasons in Abu Dhabi.

Before conducting a sensitivity analysis, it is important to determine what input variables with corresponding uncertainties

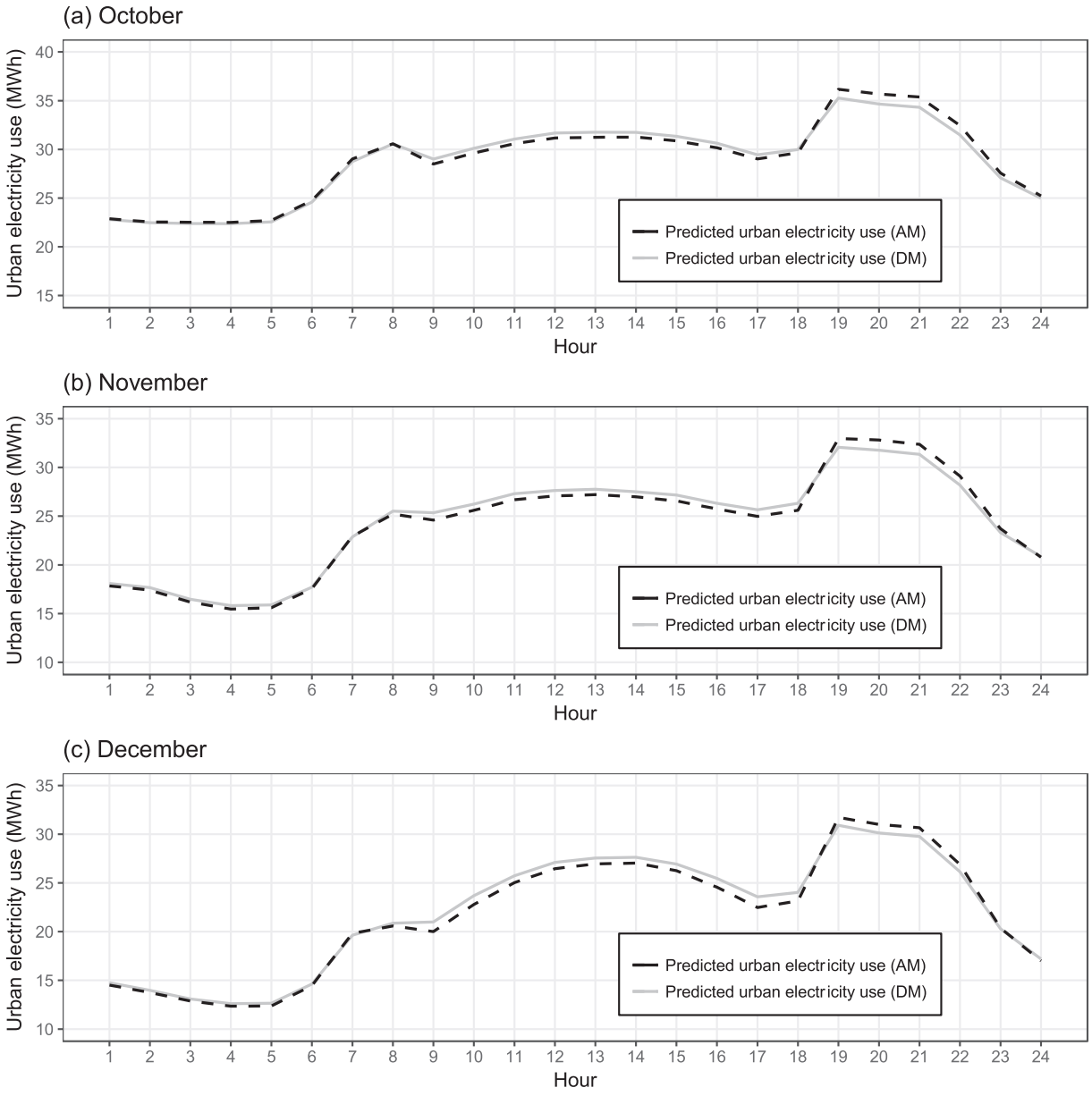


**Fig. 6.** Weekly-average diurnal profiles of the predicted urban electricity use: (a) Data between October 1 and 7, 2016; (b) Data between November 1 and 7, 2016; (c) Data between December 1 and 7, 2016.

are to be studied and what method is to be used. Defining candidate input variables with reasonable uncertainties is often an arduous task which requires a sensible engineering judgment. Selecting analysis methods with suitable sensitivity indices relies on a good mathematical understanding of the engineering system.

The objectives of this section are to create a pool of candidate inputs with uncertainties, select the Monte Carlo method for running parametric simulations, and determine the sensitivity indices needed to identify key system parameters.

### 4.1. Candidate input parameter

Based on previous studies [17,18,39] and local engineering practices [8,42–44], 30 parameters are selected and categorized into four groups for the present study (see Table 5). For the parameters in the group of meteorological factors, urban characteristics, and vegetation variables, the uncertainty ranges are intentionally defined rather broadly in order to take all the possible uncertainties into account. In terms of most building-related parameters for a specific case study, values could be obtained within relatively small uncertainty ranges from available reports and technical specifications. The corresponding values of the remaining unselected variables are taken as defaults from the data shown in Table 2. Yet, disregarding uncertain input parameters can cause a fraction of the total output uncertainty to remain unexplained in the results, which should be considered in the interpretation of the outcomes.

Uncertainty can be generally classified as *aleatory* and *epistemic* uncertainty [49]. Aleatory uncertainty refers to the inherent randomness in the system behavior, while epistemic uncertainty comes from a lack of knowledge about the appropriate value in a specific application. The parameters associated with aleatory uncertainty are assumed to have a normal distribution, which is suitable for measured physical properties. On the other hand, the

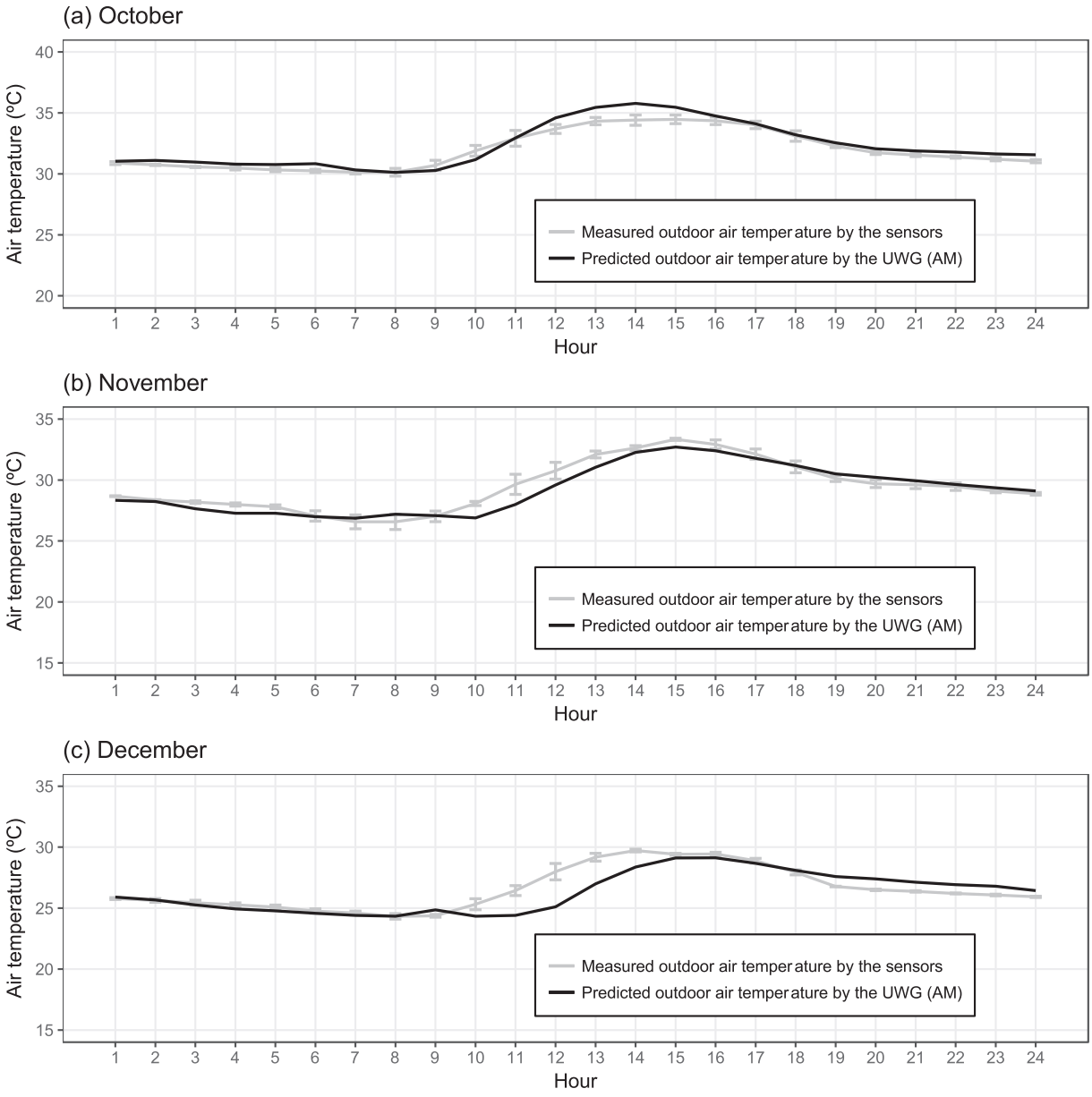


**Fig. 7.** Weekly-average diurnal profiles of the measured and predicted urban outdoor air temperature: (a) Data between October 1 and 7, 2016; (b) Data between November 1 and 7, 2016; (c) Data between December 1 and 7, 2016. The error bar represents the standard deviation of the measured urban outdoor air temperature from different sensors.

parameters associated with epistemic uncertainty are approximated with a uniform distribution, which represents that all the values are equally likely to happen. Table 5 summarizes the distribution and uncertainty for each parameter.

### 4.2. Regression-based analysis

Commonly used global SA methods in simulations include screening-based, regression-based, and variance-based methods. The technical details of these methods can be found in Refs. [23,50,51]. The selection of the SA method for a specific case study depends on many factors, such as the research purpose, the number of input parameters, the potential computational cost, etc. In particular, the regression analysis based on Monte Carlo sampling is regarded as a good practice in the global SA of built environments [31–34]. This is because the quasi-random sampling techniques can potentially offer more detailed quantitative insights into the system behavior with moderate computational costs.

As a pilot, the present study performs a global regression-based SA using the random sampling method. Technically speaking, a Monte Carlo SA provides statistical outcomes to a problem by running multiple models with a probabilistically generated input sample. These simulated results are then used to quantify the output uncertainty and calculate the sensitivity indices. As recommended by Tian [27], we implement SIMLAB [52] to automate the sampling work and use the R program [53] to conduct the uncertainty/sensitivity analysis. It is important to note that the Latin Hypercube sampling strategy is applied in this study due to its efficient stratification properties [50].

The general analysis process is structured as shown in Fig. 8. It starts by defining the distributions for aleatory and epistemic uncertainty and by producing the input samples automated via SIMLAB. Then, the sample data is read to create UWG input files via the Excel interface facilitated by MATLAB. In the meantime, the

**Table 5**
Uncertainty of the model parameters for District E3 in Abu Dhabi.

| Group | No | Parameter | Unit | Distribution | Uncertainty |
|---|---|---|---|---|---|
| Meteorological factors | A1 | Daytime urban boundary layer height | m | Uniform | 500–1000 |
| | A2 | Nighttime urban boundary layer height | m | Uniform | 50–100 |
| | A3 | Reference height of the VDM | m | Uniform | 100–200 |
| | A4 | Circulation coefficient | – | Uniform | 0.8–1.2 |
| | A5 | UCM-UBL exchange coefficient | – | Uniform | 0.1–0.9 |
| | A6 | Heat flux threshold for daytime conditions | W $m^{-2}$ | Uniform | 150–250 |
| | A7 | Heat flux threshold for nighttime conditions | W $m^{-2}$ | Uniform | 40–60 |
| Urban characteristics | B1 | Average building height | m | Normal | 35 ± 5 |
| | B2 | Fraction of waste heat into canyon | – | Uniform | 0.1–0.9 |
| | B3 | Building density | – | Normal | 0.25 ± 0.10 |
| | B4 | Vertical-to-horizontal ratio | – | Normal | 2.2 ± 0.5 |
| | B5 | Urban area characteristic length | m | Uniform | 800–1200 |
| | B6 | Road albedo | – | Normal | 0.165 ± 0.080 |
| | B7 | Traffic sensible anthropogenic heat (peak) | W $m^{-2}$ | Normal | 20 ± 5 |
| Vegetation variables | C1 | Urban grass coverage | – | Uniform | 0–0.1 |
| | C2 | Urban tree coverage | – | Uniform | 0–0.1 |
| | C3 | Vegetation albedo | – | Normal | 0.25 ± 0.05 |
| | C4 | Latent fraction of grass | – | Uniform | 0.45–0.75 |
| | C5 | Latent fraction of tree | – | Uniform | 0.5–0.9 |
| | C6 | Rural vegetation coverage | – | Uniform | 0–0.1 |
| Building systems | D1 | Glazing ratio | – | Normal | 0.5 ± 0.15 |
| | D2 | Wall U-value | W $m^{-2}$ $K^{-1}$ | Normal | 2.5 ± 1 |
| | D3 | Window U-value | W $m^{-2}$ $K^{-1}$ | Normal | 3.25 ± 1 |
| | D4 | Window SHGC | – | Normal | 0.60 ± 0.15 |
| | D5 | Infiltration rate | ACH | Uniform | 0.1–0.7 |
| | D6 | Chiller COP | – | Uniform | 2–4 |
| | D7 | Indoor air temperature set point | °C | Uniform | 20–24 |
| | D8 | Equipment load density | W $m^{-2}$ | Normal | 13 ± 3 |
| | D9 | Lighting load density | W $m^{-2}$ | Normal | 10 ± 3 |
| | D10 | Occupancy density | $m^2$ $person^{-1}$ | Uniform | 15–25 |

Note:
(a) For the parameters assumed to have a normal distribution, the uncertainty is represented as ($\mu \pm 3\delta$), where $\mu$ is the mean and $\delta$ is the standard deviation of the distribution.
(b) The parameter uncertainty is mainly assigned based on the data taken from local building design/energy codes provided by the Abu Dhabi Municipality (via personal contact), the prevailing engineering practices [8,42–44], and the previous work in Toulouse (France), Basel (Switzerland) [17,39], and Singapore [18].
(c) The physical properties of some parameters (e.g. B6 and C3) are considered according to the work by Stewart and Oke [48].
(d) Detailed physical definition of the parameters can be found in Refs. [17,39]. In particular, Ref. [17] illustrates the parameters in the rural station model and the urban canopy-building energy model, while Ref. [39] illustrates the parameters in the vertical diffusion model and the urban boundary layer model.

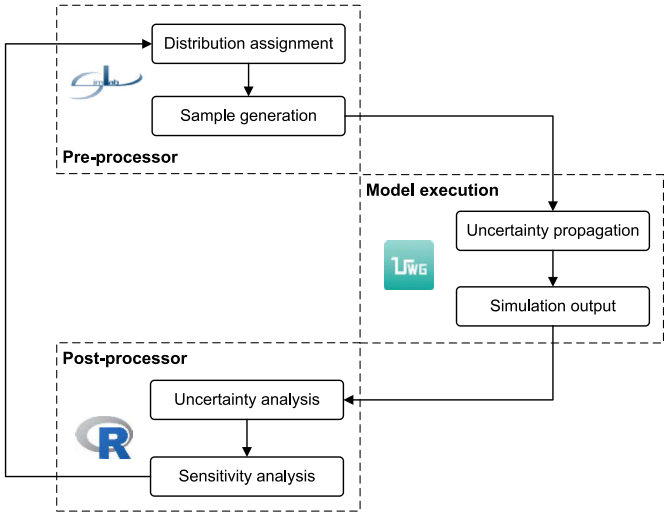


**Fig. 8.** The general process of a global sensitivity analysis using the SIMLAB, UWG, and R program.

MATLAB code checks whether any severe or fatal errors occur during the parametric simulations. Finally, the outputs are collected to quantify the uncertainty/sensitivity indices, which is supported by the R sensitivity package. In the present study, effects due to the correlation between various inputs are assumed to be negligible.

The number of parametric simulations (sample size) for a reliable Monte Carlo analysis should be large enough to ensure convergence of the sensitivity indices but not be so large as to delay the SA process. For the regression-based analysis, although nearly no formal explanation has been presented, Saltelli et al. [23] recommended the sample size of 1.5–10 times the number of input parameters. Some researchers [33,34] examined the convergence behavior with various simulation runs but gave quite different conclusions about the appropriate value. From the available experience and references, we choose to execute 1000 simulation runs for the summer and winter cases, respectively. This choice is a compromise between analysis accuracy and computational cost.

### 4.3. Sensitivity index

To estimate the sensitivity indices using the regression-based method, the model response is approximated by a multidimensional polynomial equation with a regression coefficient for each input. Then, the estimated regression coefficients are standardized using the variance of the corresponding input parameter and the variance of the model response [23]. If a first-order polynomial is chosen, we will obtain the so-called standardized regression coefficient (SRC). The absolute value of the SRC represents a measure of parameter importance, with higher SRCs indicating more impact on the model output. In addition, the sign of the SRC shows whether the model output will increase or decrease as the corresponding input changes.

Many researchers [27] have applied the sensitivity indices based on the rank transformation (SRRC) to investigate non-linear but

monotonic models. However, the rank transformation techniques would change the model during the calculation, thereby leading to the sensitivity information of a different model [23]. Such transformation would make the convergence of the sensitivity indices more difficult [33] and result in unstable outcomes. In addition, the available references indicate that the SRRC did not exhibit any outstanding performance [31,33], while the SRC could keep quite stable and in good agreement with the indices from more sophisticated global SA methods [34]. Thus, the SRC is used in the present study to interpret a quantitative measure for the influence of the inputs on the model outputs.

However, the feasibility of the SRC is limited to the model responses that can be sufficiently approximated by the fitted regression model. The SRC is not reliable when the model under investigation is highly non-linear. In order to measure how well the regression model fits the model output, we use the coefficient of determination ($R^2$). Ranging from zero to one, the coefficient of determination tests how much the variance of the model response is explained by the variance of the regression model. The larger the $R^2$ is, the better the model will fit the data. Saltelli et al. [23] have recommended a threshold of $R^2 = 0.7$ for a fairly strong regression model and its resulting SRCs.

## 5. Result and discussion

A Latin Hypercube sample matrix of size $N = 1000$ has been generated and propagated via the UWG for summer (August 1–7) and winter (February 1–7) in 2016, respectively. For each trial, the predicted hourly outdoor air temperature and daily urban electricity use were saved. The computation of a one-week scenario lasted around *one minute* on a 3.00 GHz processor computer for each trial. To the authors' knowledge, this is to date the fastest simulation engine to estimate the microclimate condition and energy consumption for a specific urban site using the physics-based modeling. Finally, corresponding indices (i.e. SRC and $R^2$) were calculated based on the generated results to enable uncertainty and sensitivity analysis.

### 5.1. Uncertainty analysis of urban air temperature

The cumulative distribution functions are used to present the results from Monte Carlo simulations and to display percentiles and confidence intervals of the outputs. Fig. 9 illustrates the uncertainty range of the weekly-average diurnal profile of the predicted outdoor air temperature in summer and winter. The shaded area represents the predicted values ranging from the 5th to 95th percentile, while the solid line represents the predicted value of the 50th percentile (i.e. median). It can be said that a model is robust enough to simulate the underlying phenomenon if, fed by the inputs with a given uncertainty, it is able to produce responses in a suitably small range. Thus, we can claim from Fig. 9 that the UWG is a fairly good simulator to approximate the thermal behavior of an urban microclimate system for different seasons with a specific degree of robustness.

It is interesting to observe that the predicted summer uncertainty band is generally larger than the winter uncertainty band, which has not been discovered before. One possible reason lies in the seasonal variation of cooling loads. During the summer in Abu Dhabi, the cooling demand becomes very high, resulting in a situation where the HVAC-related parameters may have relatively larger impacts on the variation of the microclimate. During the winter, however, the role of these parameters in the urban thermal process becomes quite trivial.

Another consequence worth noting is that the biggest uncertainty for the winter case happens during the transition period in the morning. We attribute this result to the different sets of equations that the UWG solves for daytime and nighttime periods [39], leading to physical discontinuities at the transitions. Besides, the current depiction of the mass exchange between the UBL and UCL may underestimate the impact of some factors such as the energy loss due to turbulence during the transition periods. The impact of these factors may become larger during the winter in Abu Dhabi. More attention should be paid in the future to gather better information about the corresponding components in order to reduce the output uncertainty.

### 5.2. Sensitivity analysis of urban air temperature

Based on the evaluations with a large sample size, it seems reasonable to state that 0.025 (2.5%) is a sufficient threshold for obtaining good SRC values [23,34]. Thus we decide that, for the present study, the parameter with an average of the absolute SRCs larger than 2.5% over 24 h in one day should have a significant impact on the model output. The resulting hourly coefficients of determination ($R^2$) are summarized in Table 6. The generally high $R^2$ values for most hours suggest that the higher-order effects due to non-linear behavior or parameter interaction play a fairly trivial role in the current model setting. This increases our confidence of using the SRC for the sensitivity analysis, which then identified 12 significant parameters for summer and eight for winter. Figs. 10 and 11 plot their hourly SRCs for each group respectively.

It is important to mention that no parameter in Group C (vegetation variables) is identified as a strong parameter. This can be explained by the fact that there is nearly no vegetation in Abu Dhabi, thus resulting in relatively smaller uncertainty ranges for the vegetation coverages (see Table 5). Previously, Bueno et al. [17] reported that the case study of Basel (Switzerland) is sensitive to some vegetation parameters. We should emphasize that the UHI effect seems to vary locally from one place to another and thus the parameter sensitivity needs to be considered case by case.

It can also be seen that, although all the parameters have an impact, the most critical ones are the reference height of the VDM (A3), the UCM-UBL exchange coefficient (A5), the fraction of waste heat into canyon (B2), and the nighttime urban boundary layer height (A2, for winter only). Ironically, these parameters remain the most uncertain among all the input variables. The reference height of the VDM and the nighttime urban boundary layer height are obtained from previous mesoscale atmospheric simulations [54,55] because no observations are available. The UCM-UBL exchange coefficient and the fraction of waste heat into canyon are derived from the previous literature [56] and well-educated guesses with limited domain knowledge. Since an urban system is typically characterized by a multiplicity of dynamic (building), stochastic (occupant), and probabilistic (weather) elements, it is difficult to find the exact values for these parameters for a given urban site. In order to capture the site-specific microclimate effects and reduce the uncertainty in the UWG model, additional numerical simulations of the established energy balances might be required.

Finally, the difference between the summer and winter case suggests that we should focus on different parameters when studying different periods of time. Nevertheless, the identified key factors will be the subject of our further research on the urban microclimate system in Abu Dhabi.

### 5.3. Sensitivity analysis of urban energy consumption

The same framework can yield the significant parameters influencing the daily urban electricity use in District E3, as shown in Fig. 12. The corresponding coefficients of determination ($R^2$) are 0.968 and 0.959 for summer and winter, respectively. There are 10

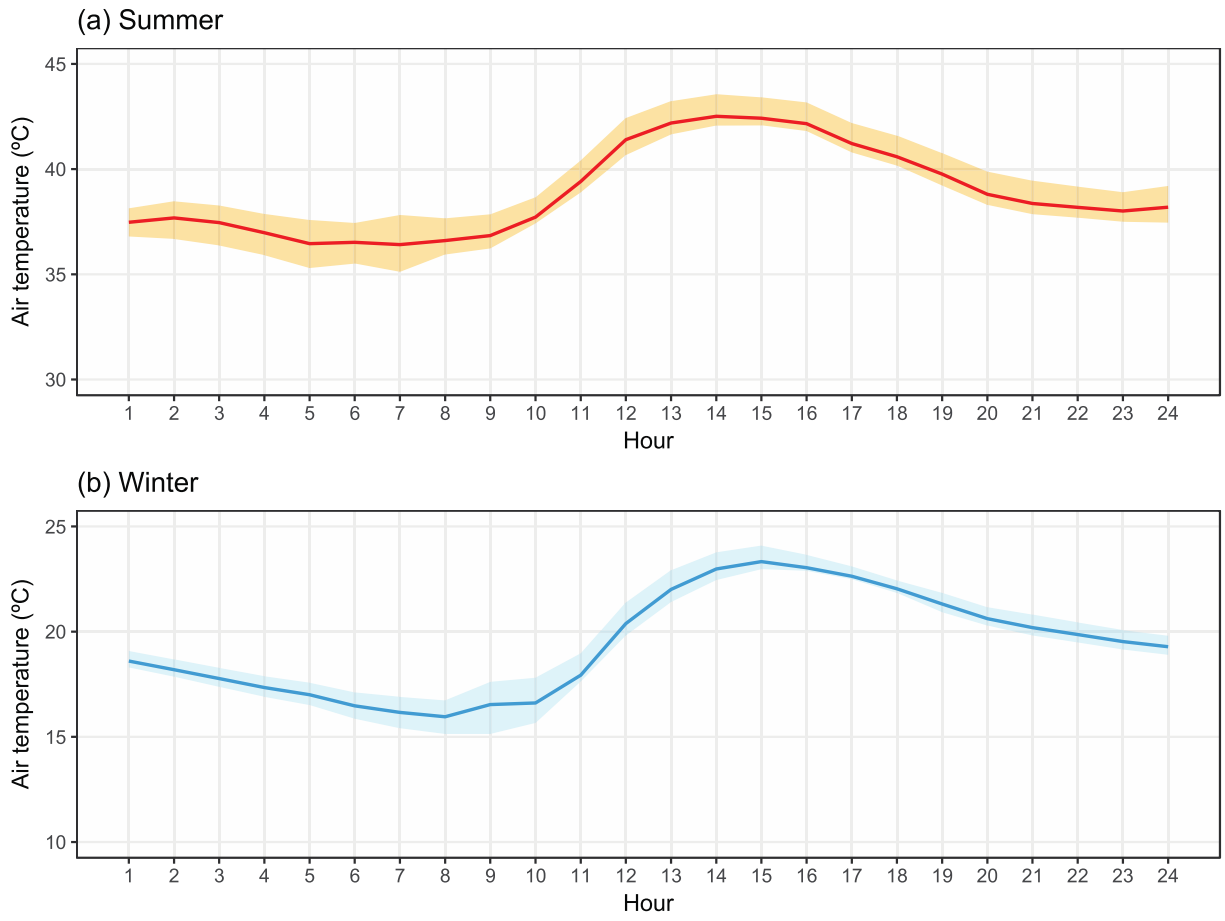


**Fig. 9.** Uncertainty range of the weekly-average diurnal profiles of the predicted urban outdoor air temperature based on Monte Carlo sampling: (a) Results between August 1 and 7, 2016 (summer); (b) Results between February 1 and 7, 2016 (winter). The shaded area represents the predicted values ranging from the 5th to 95th percentile. The solid line represents the predicted values of the 50th percentile.

**Table 6**
Coefficient of determination ($R^2$) of the regression model for the weekly-average diurnal profiles of the predicted urban outdoor air temperature.

| Hour | Summer | Winter |
|---|---|---|
| 1 | 0.637 | 0.831 |
| 2 | 0.495 | 0.850 |
| 3 | 0.540 | 0.863 |
| 4 | 0.669 | 0.877 |
| 5 | 0.798 | 0.879 |
| 6 | 0.735 | 0.868 |
| 7 | 0.834 | 0.884 |
| 8 | 0.761 | 0.892 |
| 9 | 0.829 | 0.935 |
| 10 | 0.695 | 0.902 |
| 11 | 0.784 | 0.720 |
| 12 | 0.837 | 0.814 |
| 13 | 0.755 | 0.827 |
| 14 | 0.739 | 0.814 |
| 15 | 0.707 | 0.756 |
| 16 | 0.701 | 0.717 |
| 17 | 0.750 | 0.729 |
| 18 | 0.747 | 0.778 |
| 19 | 0.786 | 0.840 |
| 20 | 0.780 | 0.802 |
| 21 | 0.744 | 0.809 |
| 22 | 0.703 | 0.819 |
| 23 | 0.634 | 0.834 |
| 24 | 0.518 | 0.853 |

strong parameters for summer and 13 for winter. Still, no vegetation-related (Group C) parameter is considered as significant for Abu Dhabi. Contrary to the case of the outdoor air temperature, most critical parameters in terms of the energy consumption are in Group D (building systems). This is because the building-related variables are directly taken into account during the energy use calculation and thus could have dominant effects.

Fig. 12 shows that the parameter sensitivities present a similar trend for summer and winter. The reason lies in the fact that there is nearly no heating mode in Abu Dhabi and only the cooling system is operated throughout the whole year to maintain the pre-determined indoor environment for the conditioned spaces. This makes Abu Dhabi a special case since it cannot provide us adequate information about our model for the heating mode during winter. However, such set of features could be fairly obtained from the previous studies in Toulouse (France), Basel (Switzerland) [17], and Boston (USA) [19].

In addition, we can see that the chiller COP (D6) dominates the energy use in summer. Due to the extremely hot weather condition in Abu Dhabi during summer, the HVAC-related energy consumption dominates other energy uses. As a consequence, the chiller COP can significantly influence the urban electricity use in summer. In winter, when the difference between the outdoor and indoor air temperatures turns smaller and the HVAC-related energy consumption becomes comparable to the remaining energy uses, other parameters (such as the indoor air temperature set point and equipment/lighting load density) start playing more important

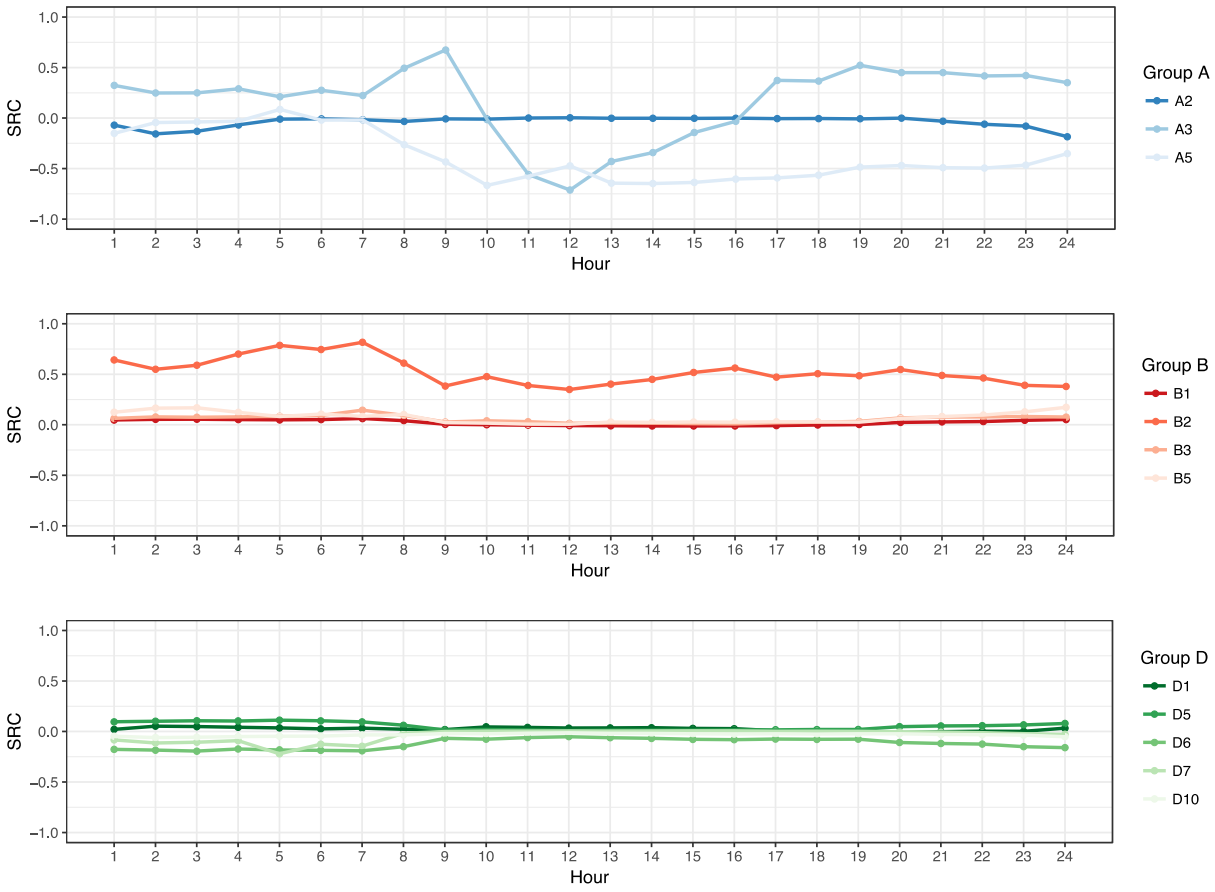


**Fig. 10.** The significant parameters obtained from the global sensitivity analysis of the weekly-average diurnal profiles of the predicted urban outdoor air temperature between August 1 and 7, 2016 (summer). The parameter denotations are the same as those defined in Table 5.

roles in altering the urban electricity use. Besides, we note that the current UWG simply implements the HVAC system without consideration of temperature-dependent COP adjustment. Constant value of the chiller COP can be critical in some cases, especially for temporal estimations under intermittent operating conditions. However, accurately characterizing the variation of chiller power with outdoor temperature requires additional modeling parameters and introduces a level of complexity that exceeds the overall character of the lumped thermal models embedded in the UWG. Thus, we consider a reasonable average value of COP, expressed as a constant, to be appropriate. Nevertheless, interpretation of the presented outcomes might be limited to some extent.

Regardless of the inherent complexity in energy management at the urban scale, the weather plays a unique and significant role since it can directly affect the thermal loads and thus the energy performances. In particular, the UHI effect can increase the cooling loads while decrease the heating loads. For tropical cities (e.g. Singapore), the UHI incurs a generally higher thermal load and thus increases the total energy cost. For temperate or heating-dominated cities (e.g. Boston), on the other hand, the UHI may be more nuanced annually since the increase in the cooling load during summer can be offset by the decrease in the heating load during winter. Nevertheless, with the overlap of increasing cooling loads in summer, the UHI can exacerbate the peak grid demand especially in extremely hot climate zones like Abu Dhabi [57].

The identification of these key factors would allow us to conduct further research to increase the accuracy of the UWG inputs, thereby reducing the uncertainties in predicting the urban energy consumption in Abu Dhabi.

## 6. Conclusion

Over the past decade, *homo sapiens* has evolved into *homo urbanus* [58]. The growing concern about urbanism motivates many research communities to expand their scope to the urban realm [59]. In the energy and environment field, some researchers are exploring how to capture at a neighborhood-to-city scale such local microclimatic phenomena as the Urban Heat Island (UHI) effect. However, modeling the urban microclimate condition comes with a big challenge since an urban system comprises very complex relationships between many elements that may overlap with each other. Thus, this study presents a deep look into an existing urban area located in Abu Dhabi (UAE) via a global sensitivity analysis method applied to an urban microclimate model.

The Urban Weather Generator (UWG) [17] is selected as the simulation engine in the present study. The UWG can be used as a physics-based model to produce the microclimate condition at the urban street level by using the meteorological information in available rural weather files. It can also be used as a bottom-up model to estimate the urban energy consumption by aggregating the building stocks. Since the previous version in 2014 [18], the UWG has been updated, especially for the urban boundary layer model and the urban canopy-building energy model. The newest version aims to make it more physically sound and more capable to handle increasingly detailed building definition.

The District E3 in downtown Abu Dhabi provides a test to the new UWG with an interesting case of heterogeneous building forms

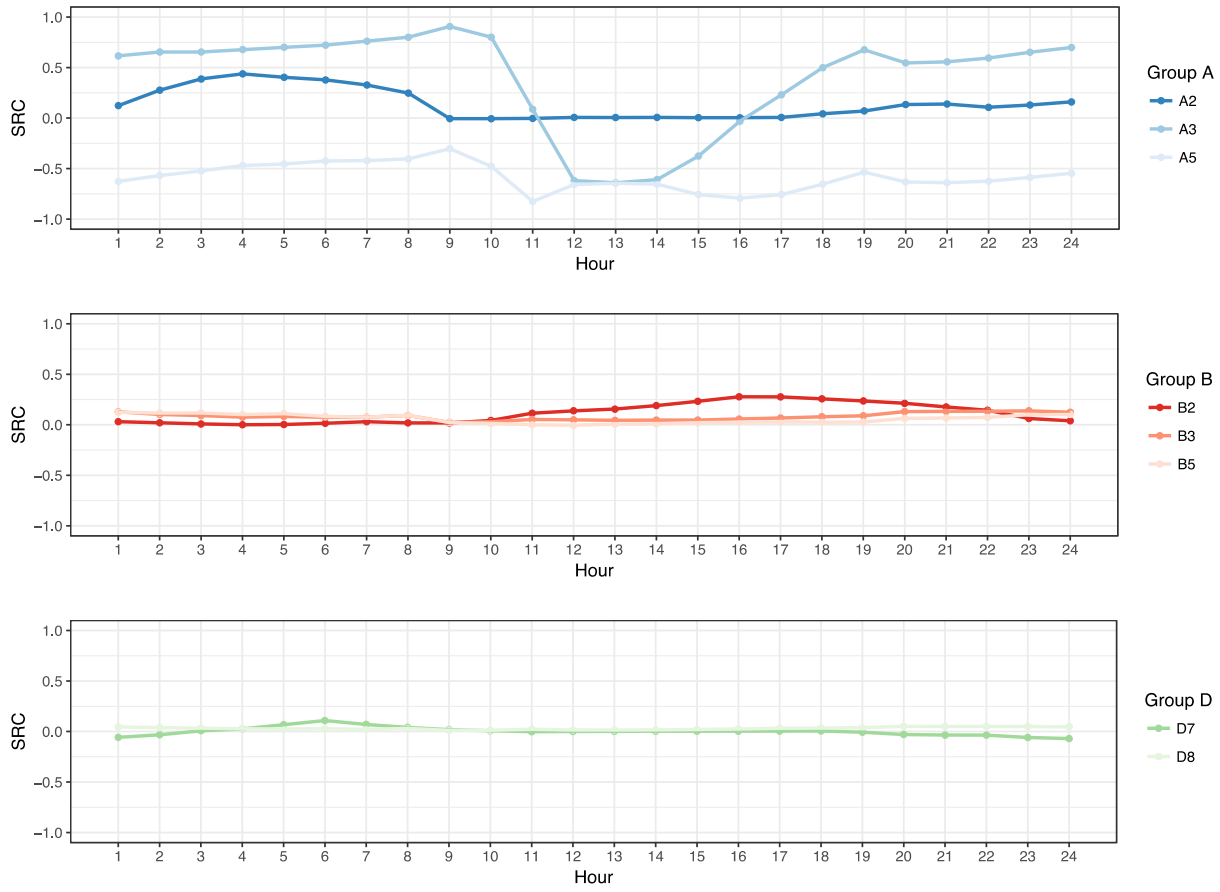


**Fig. 11.** The significant parameters obtained from the global sensitivity analysis of the weekly-average diurnal profiles of the predicted urban outdoor air temperature between February 1 and 7, 2016 (winter). The parameter denotations are the same as those defined in Table 5.

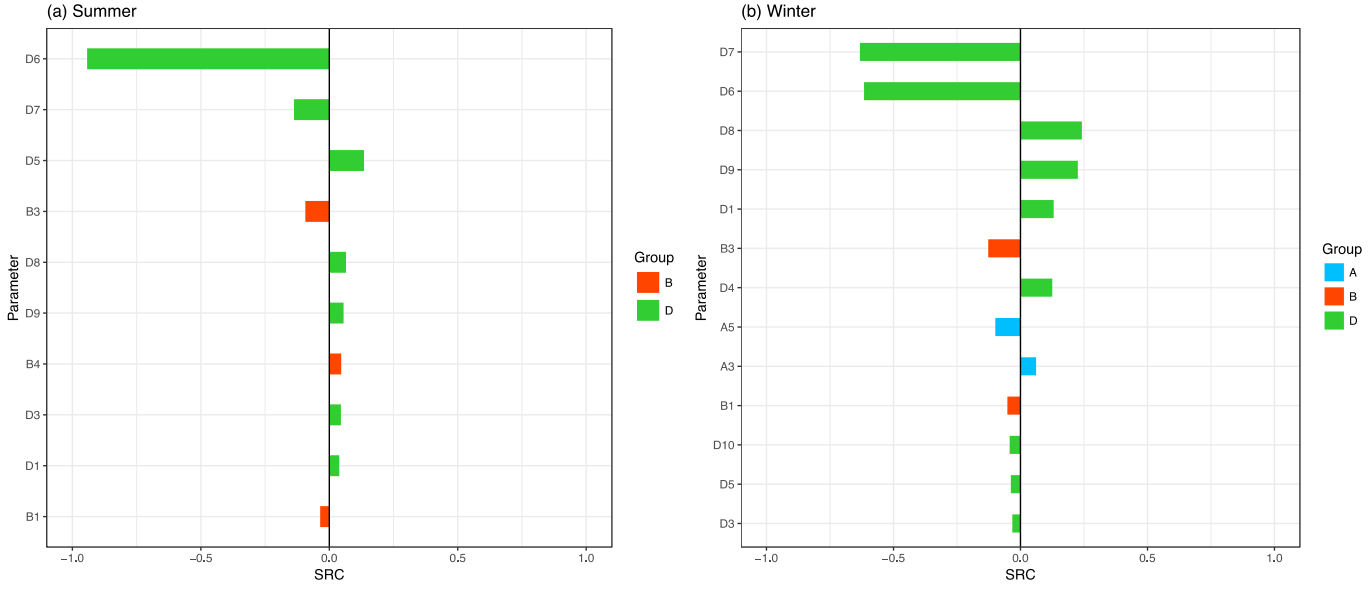


**Fig. 12.** The significant parameters obtained from the global sensitivity analysis of the predicted daily urban electricity use: (a) Results between August 1 and 7, 2016 (summer); (b) Results between February 1 and 7, 2016 (winter). The parameter denotations are the same as those defined in Table 5.

located in a tropical or subtropical climate zone. The comparison between the measurements and the predictions by a baseline model from October to December 2016 shows that the UWG can roughly capture the UHI pattern and produce some plausible values regarding the urban microclimate condition. Thus, together with previous studies [17–20], the model can be applied to different climate zones and urban configurations to yield an estimation of the UHI effect to some extent.

The regression-based analysis with Monte Carlo sampling is then used to quantify the model uncertainty and to identify significant parameters, based on 30 candidate inputs from the meteorological factors, urban characteristics, vegetation variables, and building systems. The uncertainty analysis indicates that the UWG is a fairly robust simulator to approximate the thermal behavior of the urban microclimate system in Abu Dhabi for different seasons. It is interesting to find that the predicted summer uncertainty is generally larger than the winter uncertainty, and the biggest uncertainty for the winter case happens during the transition period in the morning.

The parameter ranking based on the standardized regression coefficients (SRCs) from the linear regression suggests that no vegetation parameter has been identified as a strong parameter in Abu Dhabi. The most critical parameters are the reference height of the VDM, the UCM-UBL exchange coefficient, the fraction of waste heat into canyon, and the nighttime urban boundary layer height (for winter only). Ironically, these parameters remain the most uncertain among all the input variables, calling for further investigations into their physical mechanism. On the other hand, the most critical parameters in terms of the daily urban electricity consumption are generally associated with the building systems. In particular, the SRC of the chiller COP seems to dominate the urban energy system in Abu Dhabi during summer.

The present study has not considered the uncertainty and sensitivity of the rural measurement, which might be an interest of research in the future if sufficient data is available. In addition, future improvement of the assessment would be to conduct more detailed estimate of higher-order effects, thus revealing deeper insights into the complex parameter behavior. To incorporate the actual effect on an urban system due to occupancy, we might need to combine the UWG with reliable stochastic occupant behavior models [60]. Finally, the energy flow process modeled by the current UWG from the rural station to the urban canopy may not be a complete mechanism to depict the physics of the urban microclimate. Numerical simulations might be further needed to illustrate whether the actual interaction between the air masses in the rural and urban area has been accurately formulated for a specific city.

## Acknowledgment

This work was funded under the Cooperative Agreement between the Masdar Institute of Science and Technology, Abu Dhabi, UAE and the Massachusetts Institute of Technology, Cambridge, MA, USA, Reference Number 02/MI/MIT/CP/11/07633/GEN/G/00. The authors hereby acknowledge the Abu Dhabi Municipality for the technical support. In addition, we would like to thank Drs. Peter J. Kempthorne and Victor-Emmanuel Brunel for their advice on the uncertainty/sensitivity analysis, and thank Qinzi Luo for the discussions on the HVAC system.

## References

[1] International Energy Agency, World Energy Outlook, 2016.
[2] United Nations, Department of Economic and Social Affairs, Population Division, World Population Prospects: the 2015 Revision, Key Findings and Advance Tables, 2015.
[3] B. Obama, The irreversible momentum of clean energy, Science 355 (6321) (2017) 126–129.
[4] T.R. Oke, Boundary Layer Climates, Routledge, 2002.
[5] B.B. Hicks, W.J. Callahan, M.A. Hoekzema, On the heat islands of Washington, DC, and New York City, NY, Boundary-Layer Meteorol. 135 (2010) 291–300.
[6] S.-H. Lee, S.-U. Park, A vegetated urban canopy model for meteorological and environmental modelling, Boundary-Layer Meteorol. 126 (1) (2008) 73–102.
[7] M. Kolokotroni, X. Ren, M. Davies, et al., London's urban heat island: impact on current and future energy consumption in office buildings, Energy Build. 47 (2012) 302–311.
[8] M. Martin, A. Afshari, P.R. Armstrong, et al., Estimation of urban temperature and humidity using a lumped parameter model coupled with an EnergyPlus model, Energy Build. 96 (2015) 221–235.
[9] D.B. Crawley, Estimating the impacts of climate change and urbanization on building performance, J. Build. Perform. Simul. 1 (2) (2008) 91–115.
[10] V. Gorsevski, H. Taha, D. Quattrochi, et al., Air pollution prevention through urban heat island mitigation: an update on the urban heat island pilot project, in: Proceedings of the ACEEE Summer Study, Asilomar, CA, vol. 9, 1998, pp. 23–32.
[11] S. Oxizidis, A.V. Dudek, A.M. Papadopoulos, A computational method to assess the impact of urban climate on buildings using modeled climatic data, Energy Build. 40 (2008) 215–223.
[12] J.L. Santiago, A. Martilli, A dynamic urban canopy parameterization for mesoscale models based on computational fluid dynamics Reynolds-Averaged Navier-Stokes microscale simulations, Boundary-Layer Meteorol. 137 (2010) 417–439.
[13] V. Masson, A physically-based scheme for the urban energy budget in atmospheric models, Boundary-Layer Meteorol. 94 (2000) 357–397.
[14] R. Hamdi, V. Masson, Inclusion of a drag approach in the Town Energy Balance (TEB) scheme: offline 1D evaluation in a street canyon, J. Appl. Meteorol. Climatol. 47 (2008) 2627–2644.
[15] F. Salamanca, A. Krpo, A. Martilli, et al., A new building energy model coupled with an urban canopy parameterization for urban climate simulations – part I. formulation, verification, and sensitivity analysis of the model, Theor. Appl. Climatol. 99 (2010) 331–344.
[16] M. Roth, Review of urban climate research in (sub) tropical regions, Int. J. Climatol. 27 (2007) 1859–1873.
[17] B. Bueno, L.K. Norford, J. Hidalgo, et al., The urban weather generator, J. Build. Perform. Simul. 6 (4) (2013) 269–281.
[18] B. Bueno, M. Roth, L.K. Norford, et al., Computationally efficient prediction of canopy level urban air temperature at the neighborhood scale, Urban Clim. 9 (2014) 35–53.
[19] A. Nakano, Urban Weather Generator User Interface Development: towards a Usable Tool for Integrating Urban Heat Island Effect within Urban Design Process, SM thesis, Massachusetts Institute of Technology, 2015.
[20] J.H. Yang, The Curious Case of Urban Heat Island: a Systems Analysis, SM thesis, Massachusetts Institute of Technology, 2016.
[21] D. Coakley, P. Raftery, M. Keane, A review of methods to match building energy simulation models to measured data, Renew. Sustain. Energy Rev. 37 (2014) 123–141.
[22] The Economist, More Fall-Out from Chernobyl, June 25th, 1998.
[23] A. Saltelli, S. Tarantola, F. Campolongo, et al., Sensitivity Analysis in Practice: a Guide to Assessing Scientific Models, John Wiley & Sons, 2004.
[24] A.-T. Nguyen, S. Reiter, P. Rigo, A review on simulation-based optimization methods applied to building performance analysis, Appl. Energy 113 (2014) 1043–1058.
[25] J. Mao, Y. Pan, Y. Fu, Towards fast energy performance evaluation: a pilot study for office buildings, Energy Build. 121 (2016) 104–113.
[26] Y. Heo, R. Choudhary, G.A. Augenbroe, Calibration of building energy models for retrofit analysis under uncertainty, Energy Build. 47 (2012) 550–560.
[27] W. Tian, A review of sensitivity analysis methods in building energy analysis, Renew. Sustain. Energy Rev. 20 (2013) 411–419.
[28] T. Østergård, R.L. Jensen, S.E. Maagaard, Building simulations supporting decision making in early design – a review, Renew. Sustain. Energy Rev. 61 (2016) 187–201.
[29] I.A. Macdonald, Quantifying the Effects of Uncertainty in Building Simulation, University of Strathclyde, 2002.
[30] P. Heiselberg, H. Brohus, A. Hesselholt, et al., Application of sensitivity analysis in design of sustainable buildings, Renew. Energy 34 (9) (2009) 2030–2036.
[31] P. de Wilde, W. Tian, Identification of key factors for uncertainty in the prediction of the thermal performance of an office building under climate change, Build. Simul. 2 (2009) 157–174.
[32] B. Eisenhower, Z. O'Neil, V.A. Fonoberov, et al., Uncertainty and sensitivity decomposition of building energy models, J. Build. Perform. Simul. 5 (3) (2012) 171–184.
[33] A.-T. Nguyen, S. Reiter, A performance comparison of sensitivity analysis methods for building energy models, Build. Simul. 8 (6) (2015) 651–664.
[34] K. Menberg, Y. Heo, R. Choudhary, Sensitivity analysis methods for building energy models: comparing computational costs and extractable information, Energy Build. 133 (2016) 433–445.
[35] A.J. Arnfield, Two decades of urban climate research: a review of turbulence, exchanges of energy and water, and the urban heat island, Int. J. Climatol. 23 (1) (2003) 1–26.
[36] R. Ooka, T. Sato, K. Harayama, et al., Thermal energy balance analysis of the Tokyo Metropolitan area using a mesoscale meteorological model incorporating an urban canopy model, Boundary-Layer Meteorol. 138 (1) (2011) 77–97.
[37] C.S.B. Grimmond, T.R. Oke, Heat storage in urban areas: local-scale observations and evaluation of a simple model, J. Appl. Meteorol. 38 (7) (1999) 922–940.
[38] R.W. Fenn, S.A. Clough, W.O. Gallery, et al., Optical and infrared properties of the atmosphere, Handb. Geophys. Space Environ. (1985), 18–1.
[39] B. Bueno, J. Hidalgo, G. Pigeon, et al., Calculation of air temperatures above the urban canopy layer from measurements at a rural operational weather station, J. Appl. Meteorol. Climatol. 52 (2) (2013) 472–483.
[40] J. Hidalgo, V. Masson, L. Gimeno, Scaling the daytime urban heat island and

urban-breeze circulation, J. Appl. Meteorol. Climatol. 49 (5) (2010) 889–901.
[41] ASHRAE Handbook – Fundamentals, American Society of heating, Refrigerating and Air-conditioning Engineers. Inc., Atlanta, GA, USA, 2009.
[42] M. Deru, K. Field, D. Studer, et al., US Department of Energy Commercial Reference Building Models of the National Building Stock, 2011.
[43] H. Radhi, Evaluating the potential impact of global warming on the UAE residential buildings – a contribution to reduce the $CO_2$ emissions, Build. Environ. 44 (12) (2009) 2451–2462.
[44] A. Afshari, C. Nikolopoulou, M. Martin, Life-cycle analysis of building retrofits at the urban scale – a case study in United Arab Emirates, Sustainability 6 (1) (2014) 453–473.
[45] D.J. Sailor, A review of methods for estimating anthropogenic heat and moisture emissions in the urban environment, Int. J. Climatol. 31 (2) (2011) 189–199.
[46] A. Afshari, F. Schuch, P. Marpu, Estimation of the traffic related anthropogenic heat release using BTEX measurements – a case study in Abu Dhabi, Urban Clim. (2017), http://dx.doi.org/10.1016/j.uclim.2017.02.001.
[47] A.K. Quah, M. Roth, Diurnal and weekly variation of anthropogenic heat emissions in a tropical city, Singapore, Atmos. Environ. 46 (2012) 92–103.
[48] I.D. Stewart, T.R. Oke, Local climate zones for urban temperature studies, Bull. Am. Meteorol. Soc. 93 (12) (2012) 1879–1900.
[49] J.C. Helton, D.E. Burmaster, Guest editorial: treatment of aleatory and epistemic uncertainty in performance assessments for complex systems, Reliab. Eng. Syst. Saf. 54 (2–3) (1996) 91–94.
[50] J.C. Helton, J.D. Johnson, C. Sallaberry, et al., Survey of sampling-based methods for uncertainty and sensitivity analysis, Reliab. Eng. Syst. Saf. 91 (10) (2006) 1175–1209.
[51] C.B. Storlie, L.P. Swiler, J.C. Helton, et al., Implementation and evaluation of nonparametric regression procedures for sensitivity analysis of computationally demanding models, Reliab. Eng. Syst. Saf. 94 (11) (2009) 1735–1763.
[52] SIMLAB V2.2. Simulation Environment for Uncertainty and Sensitivity Analysis. Joint Research Centre of the European Commission. Available at: https://ec.europa.eu/jrc/en/samo/simlab.
[53] Pujol G, Iooss B, Janon A, et al. Global sensitivity analysis of model outputs. Available at: https://cran.r-project.org/web/packages/sensitivity/sensitivity.pdf.
[54] J. Hidalgo, V. Masson, G. Pigeon, Urban-breeze circulation during the CAPITOUL experiment: numerical simulations, Meteorol. Atmos. Phys. 102 (3) (2008) 243–262.
[55] X.-X. Li, T.Y. Koh, D. Entekhabi, et al., A multi-resolution ensemble study of a tropical urban environment and its interactions with the background regional atmosphere, J. Geophys. Res. Atmos. 118 (17) (2013) 9804–9818.
[56] S.R. Hanna, R.E. Britter, Wind Flow and Vapor Cloud Dispersion at Industrial and Urban Sites, vol. 7, John Wiley & Sons, 2010.
[57] L. Friedrich, P. Armstrong, A. Afshari, Mid-term forecasting of urban electricity load to isolate air-conditioning impact, Energy Build. 80 (2014) 72–80.
[58] The Economist, The World Goes to Town, May 5th, 2007.
[59] C.F. Reinhart, C.C. Davila, Urban building energy modeling – a review of a nascent field, Build. Environ. 97 (2016) 196–202.
[60] T. Hong, D. Yan, S. D'Oca, et al., Ten questions concerning occupant behavior in buildings: the big picture, Build. Environ. 114 (2017) 518–530.